Heritage Science

RESEARCH

Open Access

Bronze preservation by using composite hydrogel coating-loaded corrosion inhibitors

Sheng Zhou[1], Zongshen Zhao[1], Heyi Mao[1], Lei Wang[1], Junyin Chen[2], Jiachang Chen[3*] and Xia Huang[1*]

Abstract

Bronze has been used for various applications since ancient times, and therefore, its preservation is critical. However, preserving bronze is challenging. The traditional inhibitor sealing method is limited by its toxicity and sealing effects. In this study, a benzotriazole (BTA) inhibitor loaded with a composite hydrogel of sodium alginate and cyclic-peptide-grafted β-cyclodextrin was prepared. The chemical structure of the components of the composite hydrogel coating was characterized through Fourier-transform infrared spectroscopy. The microstructure of the coating on bronzeware was characterized through scanning electronic microscopy. The thermal analysis of the composite hydrogel coating confirmed that BTA was introduced successfully into the composite hydrogel, and the coating exhibited the liquid crystalline property because of the mesogenic unit—cyclic peptide. Electrochemical impedance spectroscopy revealed that the modified β-cyclodextrin-loaded benzotriazole considerably improved the corrosion resistance. In a certain range, the higher was the BTA-loaded Cyc-g-β-CD ratio, the stronger was the protective effect of the gel coating. In conclusion, corrosion inhibitors can considerably improve the corrosion resistance of gel coatings.

Keywords: Bronzeware preservation, Composite coating, Cyclic peptide-g-β-CD, Corrosion inhibitor

Introduction

Bronze has been used extensively throughout the history of mankind. Therefore, bronzeware forms a critical part of cultural heritage. However, rusting of the surfaces of most bronzeware is inevitable. Corrosion can be categorized into two types, namely overall (microcell corrosion that can be described as extremely tiny electrodes) and small-pore (corrosion that occurs from outside to inside). Benzotriazole (BTA) is a commonly used corrosion inhibitor [1–3].

Direct application of corrosion inhibitors on bronze surfaces results in sublimation because of the presence of vapor pressure, and under long-term storage, a layer of crystals forms on bronze surfaces. BTA can not only react with bronze rust but also darken the bronze surfaces because of excessive oxidation, which is undesirable [4].

At present, researchers have realized a variety of methods to load corrosion inhibitors into protective coatings, enabling them to have more effective corrosion inhibition capabilities. Martina et al. developed active coatings based on layered double hydroxide nanocarriers loaded with 2-mercaptobenzothiazole (MBT) to protect bronze surfaces from corrosion, and overcome the shortcomings of corrosion inhibitors that are easily degraded by light, making the coating have a lasting anti-corrosion effect [5]. Dr. Ma et al. used nano-additives filled with corrosion inhibitors to modify organic coatings [6]; Dr. Fu et al. prepared an intelligent anticorrosion coating based on the mechanized hollow mesoporous silica nanoparticles (HMSs) [7]; Mikhail et al. realized the intelligent self-healing ability of the protective coating by incorporating layer-by-layer (LbL) assembled nanoreservoirs of corrosion inhibitor [8].

*Correspondence: chenjiachangbaohu@163.com; happyhxia@163.com

[1] School of Materials Science and Engineering, Zhengzhou University, Zhengzhou, Henan 450001, People's Republic of China
[3] Henan Provincial Institute of Cultural Relics and Archaeology, Zhengzhou, Henan 450000, People's Republic of China
Full list of author information is available at the end of the article

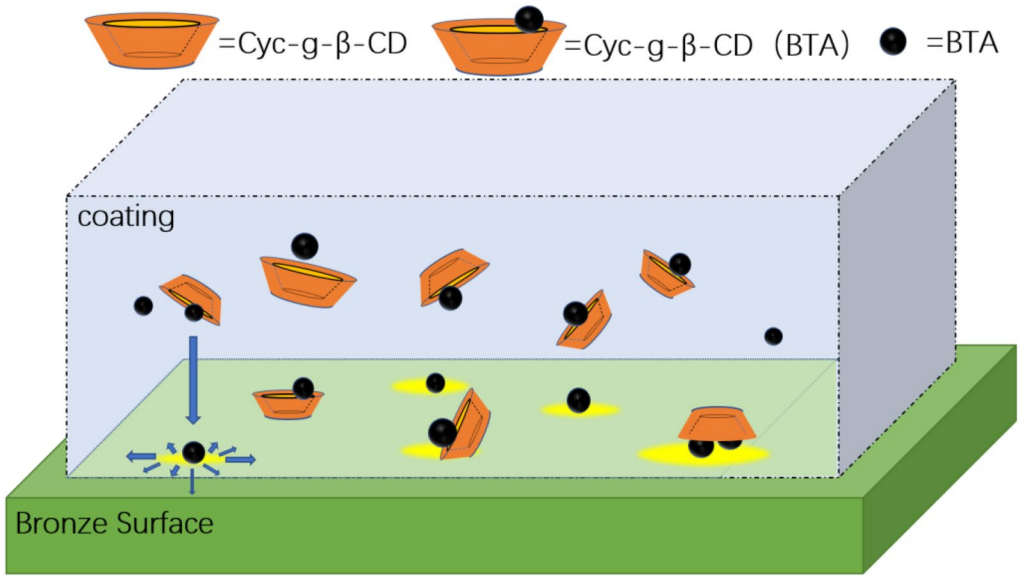

Scheme 1 Mechanism of Cyc-g-β-CD (BTA) action on the bronze surface

Among them, the method of corrosion inhibitor loading on polymer hydrogels has attracted considerable research attention. Hydrogel coating-loaded corrosion inhibitors can effectively reduce corrosion inhibitor loss and help preserve the appearance of bronzeware. Hydrogel performance is affected by factors such as environmental response, biocompatibility, and drug release [9]. Importance of hydrogels for corrosion protection is gradually being recognized. Ren et al. developed an intelligent corrosion inhibitor with enhanced corrosion protection in acidic environments using photo-crosslinked poly (DMAEMA) hydrogels as benzotriazole carriers [10]. The results indicated that the intelligent corrosion inhibitor can provide the unique advantage of protecting copper corrosion in the long term due to the highly sustained BTA supply. Gu et al. were the first to use polyvinyl alcohol (PVA) hydrogels loaded with modified polyepoxysuccinic acid (PESA) and imidazoline to prevent corrosion on metal pipelines in oil fields [11].

However, a limitation of this method is that it does not provide the effective encapsulation and release of corrosion inhibitors. According to the international principles of protection (Principles of preservation status quo and reversibility), protective coatings must not only be durable but also allow reprocessing. Therefore, degradable polymer coatings were proposed to achieve reprocessing of coatings. Degraded conditions can cause varying degrees of damage to fragile bronze equipment.

Therefore, in the present study, cyclodextrin was used as the corrosion inhibitor carrier. β-Cyclodextrins contain a hydrophobic inner cavity and a hydrophilic outer cavity. Based on host–guest interactions, β-cyclodextrins are commonly used to encapsulate the most widely used guest molecules [12]. Previously, a novel graphene-based polymer/β-cyclodextrin supramolecular nanocontainer, with excellent inhibitor encapsulation ability and high permeation resistance, was synthesized [13], which indicated that nanocontainers loaded with corrosion inhibitors provide excellent passive and active corrosion resistance to the coating system.

We introduced amino-acid-derived cyclic peptides in the cyclodextrin to exploit the strong adsorption capacity of cyclic peptides on bronze substrates [14]. For the liquid crystallinity of cyclic peptides, rearrangement occurs during the post curing placement. Such controllable rearrangement during aging is beneficial for the nondestructive peeling of coatings and can provide effective protection during the working period and nondestructive stripping after failure. The mechanism of Cyc-g-β-CD (BTA) action on the bronze surface is displayed in Scheme 1. As the carrier of BTA corrosion inhibitor, cyclodextrin can release its loaded BTA when it is in contact with the copper substrate, thus inhibiting corrosion.

To overcome the mechanical limitations of single-component cyclodextrin gels, we used the composite hydrogels of alginate with modified cyclodextrin.

Sodium alginate (SA) is a natural nontoxic hydrogel material that can undergo simple ionic cross-linking to form hydrogels. It is a promising polymerization material among all hydrogel-coating materials because it is chemically active, nontoxic, odorless, and environment-friendly and contains abundant carboxyl and hydroxyl

groups. Moreover, the mechanical strength of SA can be improved and new adsorptive functional groups can be generated through physical and chemical modification methods [15].

More specifically, we studied a new composite coating method and attempted to load BTA with Cyc-g-β-CD and investigated its corrosion inhibition effect on bronze sheets.

Materials and methods

Materials

β-Cyclodextrin (purity > 98%) and BTA (analytically pure) were obtained from Shanghai Macklin Biochemical Co., Ltd. p-Toluenesulfonyl chloride (purity > 99%), sodium hydroxide (96%), hydrochloric acid (37%), ethanol (purity > 99.5%), calcium carbonate (99.5%), ammonium hydroxide (2.00 N), and SA (analytically pure) were obtained from ALADDIN. Acetone (analytically pure) and ethylenediamine (analytically pure) were obtained from Tianjin Fuyu. Deionized water was used for all experiments.

Methods

Infrared analysis

Fourier-transform infrared spectrometry (FTIR) was performed using Nicolet IS10. Because water may be contained in the specimen, the test samples should be adequately dried before grinding the specimen to a powder form, and the specimen should be prepared under an infrared lamp to avoid water uptake by potassium bromide and specimen. The beam wavenumber range of 4000–500 cm^{-1} was used for testing aminoacylated β-cyclodextrins, Cyc-g-β-CD, and Cyc-g-β-CD (BTA) to analyze β-cyclodextrin modification and the behaviors of corrosion inhibitors. Mineralized bronze sheets coated with SA hydrogel, mineralized bronze sheets coated with BTA-loaded Cyc-g-β-CD /SA composite coating, and BTA-loaded Cyc-g-β-CD /SA composite coating were measured in the total reflection mode.

Thermal analysis

PYRIS 1 thermogravimetric (TGA) analyzer (Perkin Elmer, USA) was used to obtain the differential scanning calorimetry (DSC) curves of the samples. Under nitrogen atmosphere, the initial temperature was 35 °C, the heating rate was 10 °C/min, and the termination temperatures were 160 °C and 360 °C, respectively.

Scanning electron microscopy

A tungsten filament benchtop scanning electron microscope (QUANTA 650) was used to observe surface morphologies of the composite coating and bronze binding sites, as well as the gel coating on the surface of bronze. The working voltage was 15 kv, and the working mode was the secondary electron mode.

Electrochemical tests

The traditional three-electrode system comprising reference (saturated calomel), working, and auxiliary electrodes (platinum electrode) was used in the experiment to monitor the corrosion potential of the studied electrode. The frequency range was 0.01–100 k Hz, and the AC amplitude was 5 mV. The corrosion potential of the electrode to be studied was calculated after stabilization post immersion for half an hour. The measurement results are expressed in terms of Nyquist plots or Bode plots for obtaining useful electrochemical information for the relevant evaluation of the corresponding coatings versus the substrate [16, 17].

Artificial aging test

To evaluate the long-term protective effect of the coatings, the coated and uncoated bronze sheets in closed glass containers were heated at 50 °C in the presence of hydrochloric acid vapor (1.0 M HCl in water) and 100% relative humidity [18]. The sheets were then subjected to the 60-h accelerated corrosion tests, and the electrochemical analysis of bronze sheets before and after corrosion was performed.

Experiment

Preparation of Cyc-g-β-CD

Amide modification of β-cyclodextrin

White powdered β-cyclodextrin was dissolved in deionized water. The solution was placed in a mechanical stirrer (Zhongda Instrum tech GmbH, Jiangsu, China) and stirred until an emulsion was obtained. Next, 1 mol/L sodium hydroxide solution was added to a flask containing β-cyclodextrin, and the mixture was stirred well for 1.5 h. Stirring was continued for 3 h under an ice water bath at 0 ℃, and p-toluenesulfonyl chloride was added in three batches. After stirring, insoluble matter was separated and filtered. The resulting filtrate was placed into the beaker to adjust pH to approximately 7 with diluted hydrochloric acid. At this stage, numerous white precipitates appeared in the beaker. The precipitates were collected through suction filtration following precipitation and then dissolved in boiling water to remove insoluble material through hot filtration. The filtrate was again allowed to stand for 12 h in cold storage at 0 ℃ to allow recrystallization. After complete precipitation and suction filtration, a white solid was obtained, which was recrystallized twice from distilled water. Thereafter, the white solids were vacuum dried in a vacuum drying oven (Shuli instrument GmbH, Shanghai, China) at 60 ℃ for 12 h to obtain sulfonylated β-cyclodextrins. Afterward,

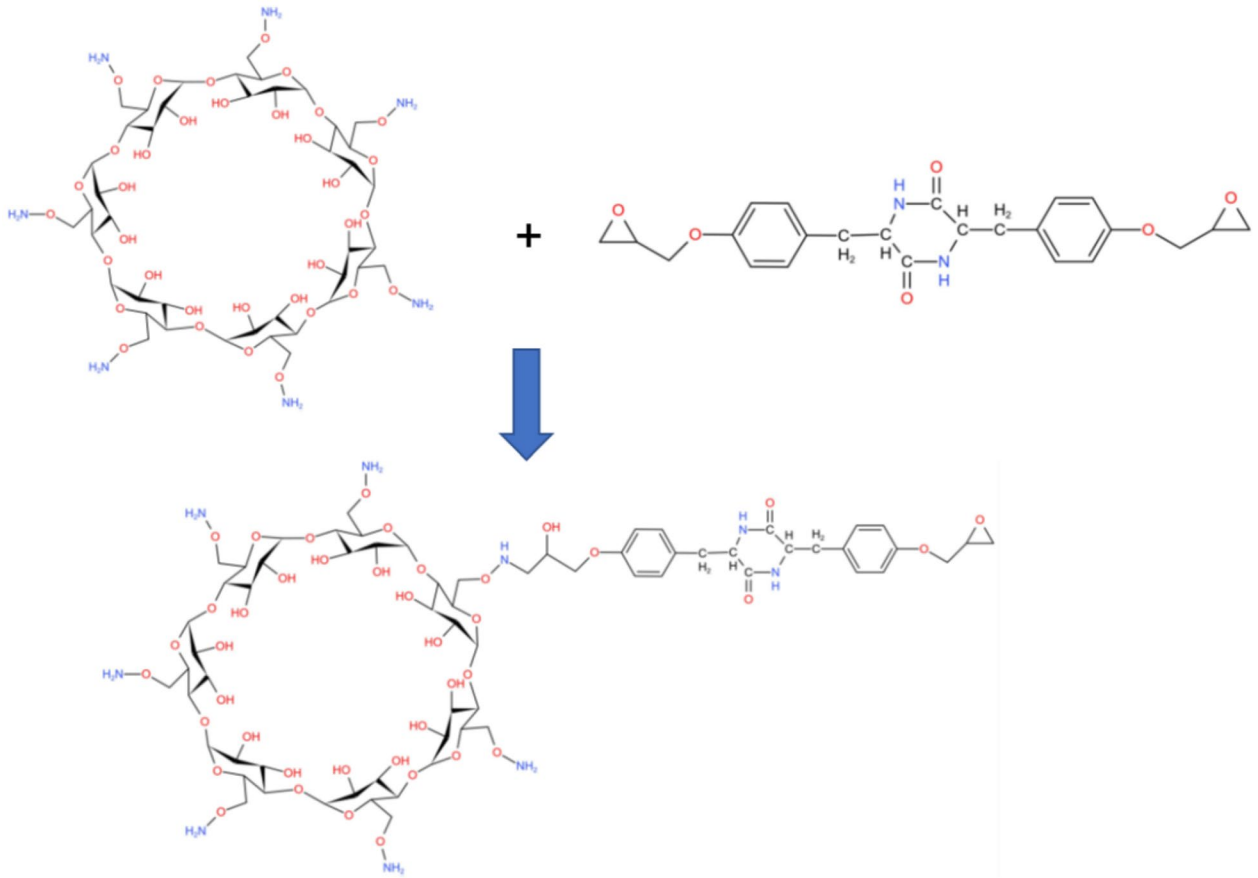

Scheme 2 Synthesis of cyclic peptide-grafted β-cyclodextrins (Cyc-g-β-CD)

3 g of the sulfonylated ring paste was placed into a flask. Subsequently, 15 mL of ethylenediamine was added to the flask and then allowed to react under a water bath at a constant temperature of 70 ℃ for 4 h. The resultant solution was quickly mixed with 400 mL of acetone. Suction filtration was performed to obtain a pale-yellow solid. After performing washing filtration with acetone thrice, the obtained pale-yellow solid was vacuum dried in a constant-temperature vacuum drying oven at 50 ℃ for 48 h. After removal, the obtained solid was dissolved in deionized water at a mass ratio of 1:5 and lyophilized in a freeze dryer (Xinzhi biotechnology GmbH, Ningbo, China) to obtain amino-modified β-cyclodextrin.

Synthesis of Cyc-g-β-cyclodextrins

Epoxide Cyc [19] (lab made) was mixed with amino-modified β-cyclodextrin in a molar ratio of 1:1 and dissolved in deionized water. The mixture was placed on a thermostatically heated magnetic stirrer under a constant temperature of 50 ℃ for 5 h, followed by freeze drying and lyophilization to obtain cyclic-peptide-grafted β-cyclodextrins (Cyc-g-β-CD), as displayed in Scheme 2.

Preparation of BTA-loaded Cyc-g-β-CD

The synthesized Cyc-g-β-CD containers (10 mg/mol) were mixed with ethanol solution containing BTA (50 mg/mol) and stirred in vacuum for 8 h to render the solution fully inclusive. Ethanol was distilled out at 80 ℃, the distilled solution was lyophilized by placing it in a freeze dryer, and BTA-loaded containers were obtained after removal.

Preparation of BTA-loaded Cyc-g-β-CD /SA composite coating

First, 100 mL of deionized water was added to a beaker. Then, 1 g of SA weighed using an electronic balance was placed on a constant-temperature heating magnetic stirrer, and the solution was magnetic stirred for 3 h to achieve complete solubilization of SA in water. Next, 100 mg of benzotriazole-loaded epoxy-modified β-cyclodextrin was weighed using an electronic balance (Hengji Scientific Instruments, GmbH, Shanghai, China) and added directly to the SA solution. The beaker was allowed to sonicate for 30 min in an ultrasonic cleaner (Jiemeng Washing equipment GmbH, Shenzhen, China)

and then removed. Afterward, it was placed back on a magnetic stirrer and vigorously stirred for 1.5 h to obtain a homogeneous solution. Calcium carbonate was added to the solution with vigorous stirring for 30 min after ultrasonication for 20 min to ensure complete dispersion. The solution was sealed using a tin foil paper and placed on a shelf to stand for a certain time to allow complete gelation.

Mineralization of bronze sheets

Washing and cleaning of the smeary surface of bronze flakes were performed by dissolving ammonia and hydrochloric acid in a 1:1 ratio in water. The sheared bronze sheets were placed in the coordinated solution for 8 h and then air dried to obtain mineralized bronze sheets.

Coating on bronze platelets

The obtained gel was coated onto the surface of bronze sheets by brushing (each bronze sheet gauge was 1 cm × 2 cm, and 1 mL of the obtained gel was coated per face). After drying at 35 °C for 12 h, the flakes were prepared for subsequent characterization.

Results and discussion

Chemical structure analysis of composite coating

For amide β-cyclodextrins, the appearance of a strong and broad peak at 3500 cm^{-1} was attributed to O–H stretching vibration. The weak peak observed at 1583 cm^{-1} is a characteristic of the benzene ring skeleton (C=C), and the peak at 1660 cm^{-1} is a characteristic of amide bonds. The appearance of these characteristic peaks confirmed the successful modification of the amino groups of β-cyclodextrin molecules. After the ring opening amination of CDs with Cyc, amide bonds and secondary amide were introduced, and a C=O absorption peak was observed at 1650 cm^{-1}. The observation of the thiazole ring peak at 1247 cm^{-1} and N–H absorption peaks at 1355 and 1460 cm^{-1} proved that BTA was successfully loaded in the modified β-cyclodextrin molecule (Fig. 1).

Mineralized bronze sheets coated with SA/Cyc-g-β-cyclodextrin hydrogel showed sharp peaks at 1660 cm^{-1} and 1030 cm^{-1}, indicating that Cyc-g-β-CD (BTA) was effectively doped in the SA hydrogel (Fig. 2). The comparison of FTIR spectra of mineralized bronze sheets coated with BTA-loaded Cyc-g-β-CD/SA composite coating and SA/ Cyc-g-β-Cyclodextrin hydrogel shows the fingerprint region of mineralized bronze sheets coated with BTA-loaded Cyc-g-β-CD/SA composite coating appears red shift. The FTIR of mineralized bronze sheets coated composite coating showed two peaks at 3460 cm^{-1} and 3300 cm^{-1}, whereas uncoated composite coating only showed a strong and wide peak at 3460 cm^{-1}. This is because the released BTA reacts with the bronze matrix and produces supramolecular forces.

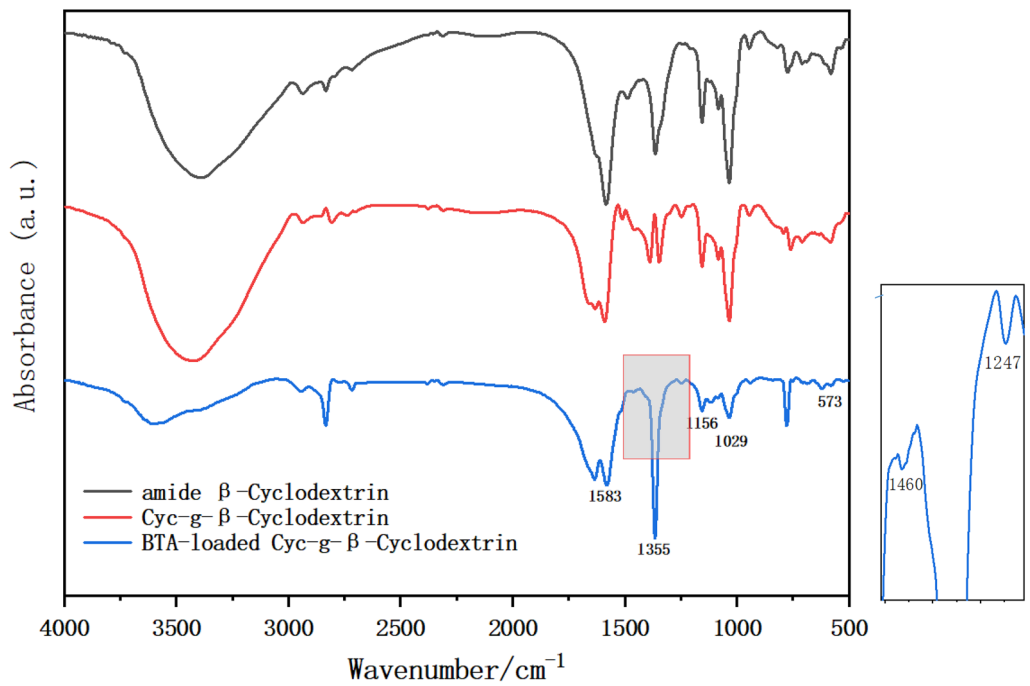

Fig. 1 DSC curves: **a** BTA; **b** Cyc-g-β-CD and BTA-loaded Cyc-g-β-CD

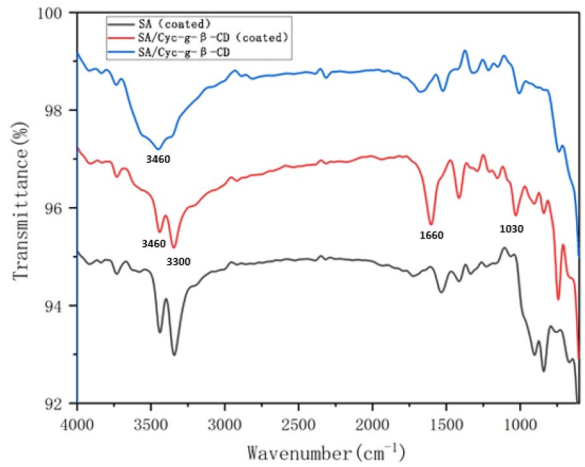

Fig. 2 FTIR spectra of mineralized bronze sheets coated with SA hydrogel, mineralized bronze sheets coated with BTA-loaded Cyc-g-β-CD /SA composite coating, and BTA-loaded Cyc-g-β-CD /SA composite coating

Thermal analysis of composite coating

As shown in Fig. 3a, the melting peak of BTA was approximately 115 ℃.

The DSC curve of Cyc-g-β-CD exhibited a melting peak at approximately 100 ℃ and two upward endothermic peaks in the temperature ranges of 210–240 ℃ and 300–320 ℃. The two upward peaks implied the presence of solidifying cross-links. Compared with the findings on cyclodextrins reported in the literature [20], there were obvious differences in melting point and cross-links endothermic peaks, which implied that the introduction of Cyc changed the condensed structure of cyclodextrins.

In the DSC curve of BTA-loaded Cyc-g-β-CD (Fig. 3b), the melting peak of BTA could not be observed, but a new endothermic peak was observed between the melting peaks of BTA and Cyc-g-β-CD. The corresponding enthalpy also increased from 197 uVs/mg to 212 uVs/mg. Moreover, BTA-loaded Cyc-g-β-CD exhibited only one cross-linked exothermic peak, which was located between the two exothermic peaks of the unloaded BTA sample. The aforementioned results indicated the presence of a strong intermolecular interaction between BTA and cyclodextrin, which lead to the formation of a thermodynamically compatible system.

Microtopography of composite coating on bronze surfaces

The microtopography of the surface of the gel-coated mineralized bronze sheets was analyzed through SEM. Figure 4 displays the surface SEM images of the mineralized bronze sheets coated with BTA-loaded Cyc-g-β-CD/SA composite hydrogel.

Macroscopically, a gel coating formed films and combined with mineralized bronze. Figure 4b, c, and d reveal the agglomeration distribution of liquid crystalline domain formed by liquid crystalline motifs. This texture appeared because mineralized bronze affects the liquid crystal arrangement in the coating, which indicated an excellent interaction between the coating and bronze. Because of liquid crystallinity of epoxy Cyc, the Cyc-g-β-CD containers dispersed well in the coating, and the presence of lamellar liquid crystals also enhanced the barrier properties of the gel coating to some extent.

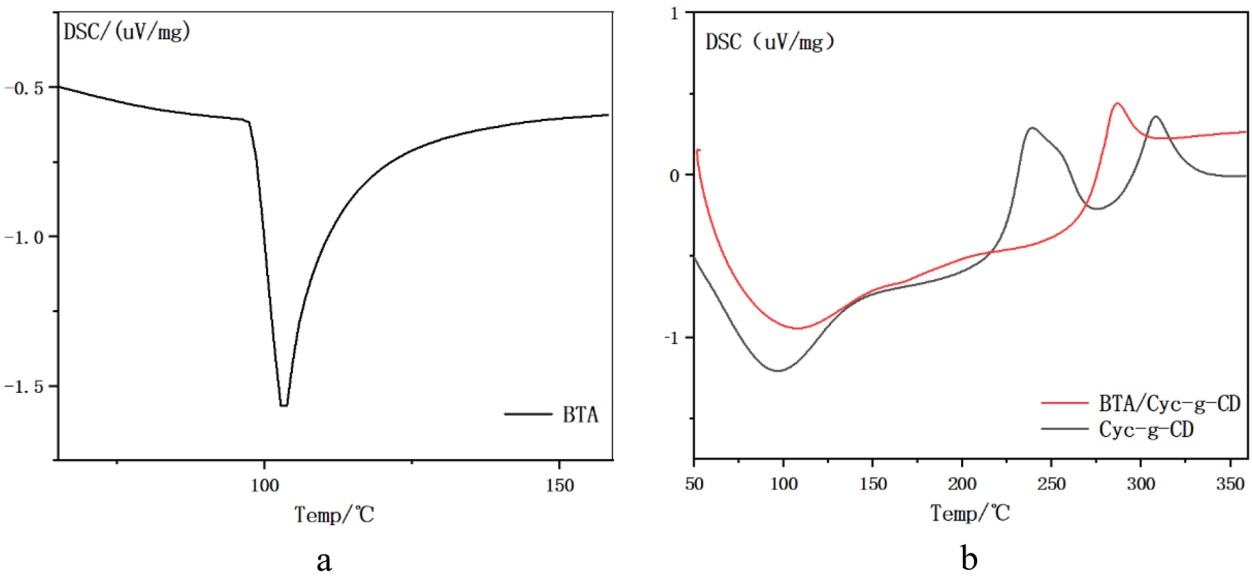

Fig. 3 FTIR spectra of amide β-cyclodextrin, Cyc-g-β-cyclodextrin, and BTA-loaded Cyc-g-β-cyclodextrin

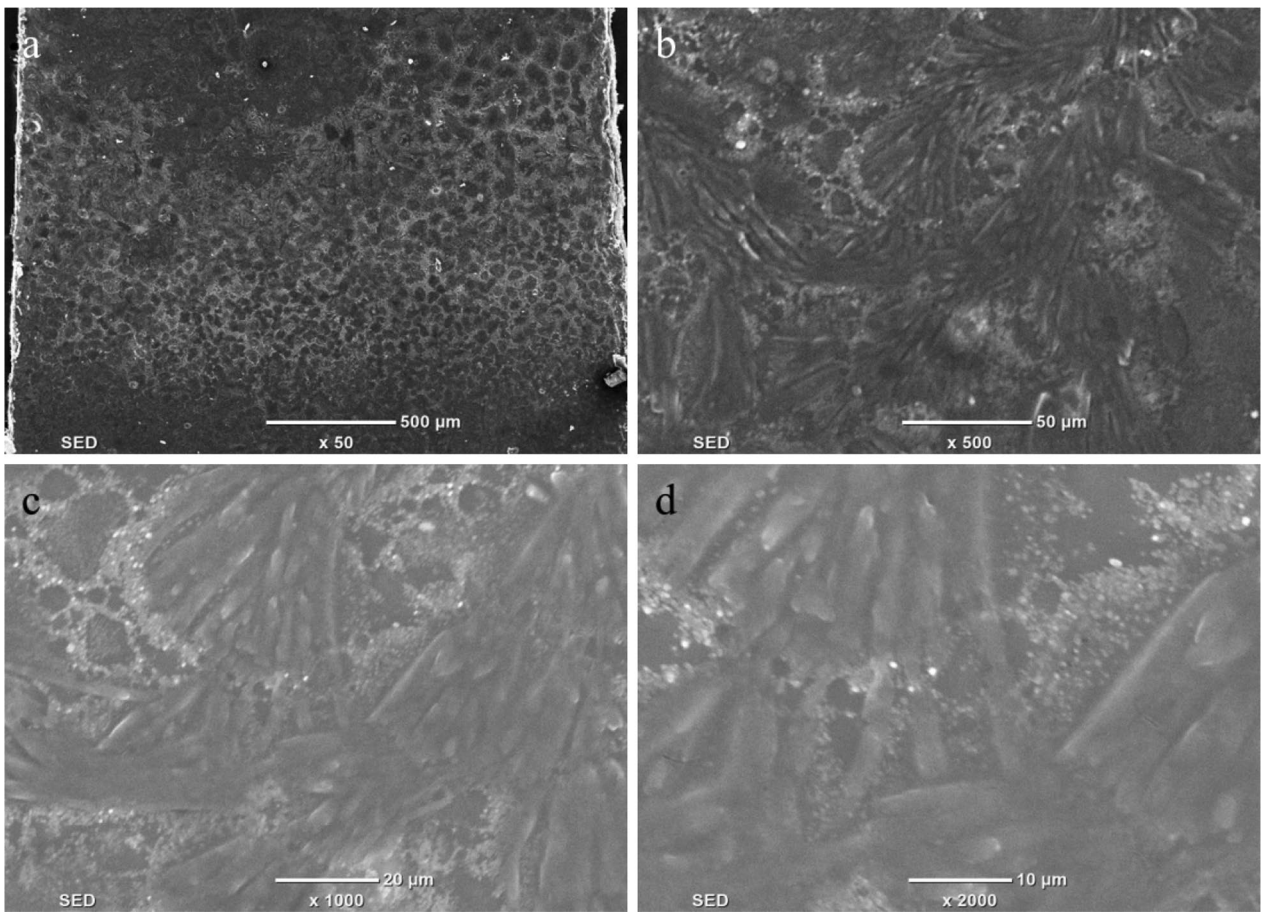

Fig. 4 Scanning electron microscopy (SEM) images of the gel-coated mineralized copper bronze sheet surface at various magnifications. Scale bars in a, b, c, and d are 0.25, 0.25, 0.2, and 0.2 cm, respectively; **a** Surface SEM images at a magnification of 50X; **b** 500X; **c**, 1000X; and **d** 2000X

Figure 5 displays the SEM images of the cross-section of mineralized copper bronze sheets coated with BTA-loaded Cyc-g-β-CD/SA composite hydrogel. As shown in Fig. 5a, the gel coating and mineralized bronze surface combined well, and the thickness of the gel coating was approximately 1 µm. The crack between coating and bronze surface was approximately 2 µm. The presence of cracks revealed that there were physical bonding between the coatings and bronze, which implied that the composite coating was removable. The appearance of the cracks could be attributed to dryness inside or improper operation when intercepting the section.

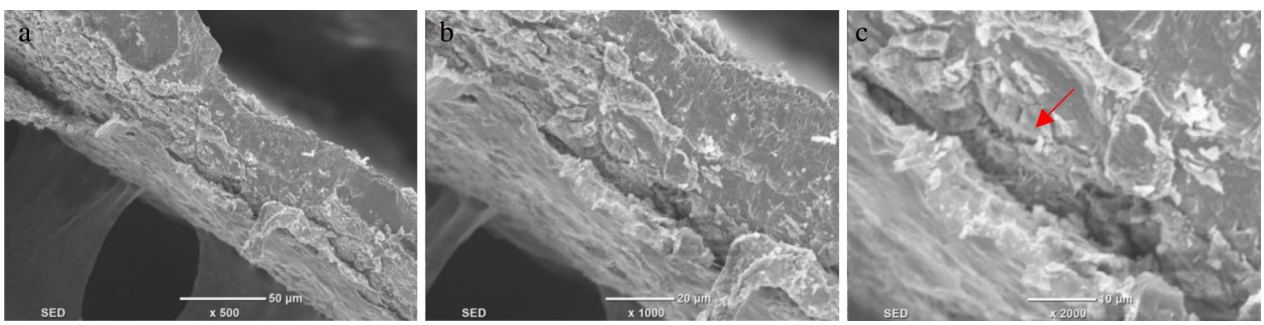

Fig. 5 SEM images of the cross-section of the gel-coated mineralized copper bronze sheet at various magnifications; scale bars in a, b, and c are 0.25, 0.2, and 0.2 cm, respectively; **a** Surface SEM images at magnifications of **a** 500X; **b**) 1000X; and **c** 2000X

The coating was highly integrated with mineralized bronze, and the inlay was stable because gel coating fluidity can occupy the pits on the surface of mineralized bronze and rust-induced voids. The released BTA [21] can react with the bronze matrix [22], and the final gel coating could stud onto mineralized copper.

Electrochemical test of composite coating on mineralized copper bronze

Electrochemical methods were used to study the modification of alginate-based benzotriazole-loaded β-cyclodextrin composite coatings on the protective properties of mineralized bronze. SA-based, benzotriazole-loaded Cyc-g-β-CD composite coatings were coated onto the mineralized bronze sheet electrode surfaces and immersed in a 3.5% NaCl solution for electrochemical AC impedance tests. The obtained results are displayed in Fig. 7 [23].

Figure 6 displays the Nyquist, Bode, and phase diagrams of the bare mineralized bronze sheet electrode immersed in 3.5% NaCl solution. Figure 7 shows Nyquist plots, Bode plots, and phase plots for the alginate-based benzotriazole-loaded Cyc-g-β-CD composite coating soaked in 3.5% NaCl solution.

Compared with those displayed in Fig. 6, the Cyc-g-β-CD composite coating with SA-based benzotriazole exhibited a considerable increase in the radius of electrode impedance arc, and the maximum value of the obtained phase angle considerably improved, which indicated that the SA-based benzotriazole-loaded Cyc-g-β-CD composite coating offered a certain protection to the mineralized copper organelle sheets against corrosion.

Because of the flake liquid crystal and the network structure inside the gel, SA-based benzotriazole-loaded Cyc-g-β-CD composite hydrogels can directly form a

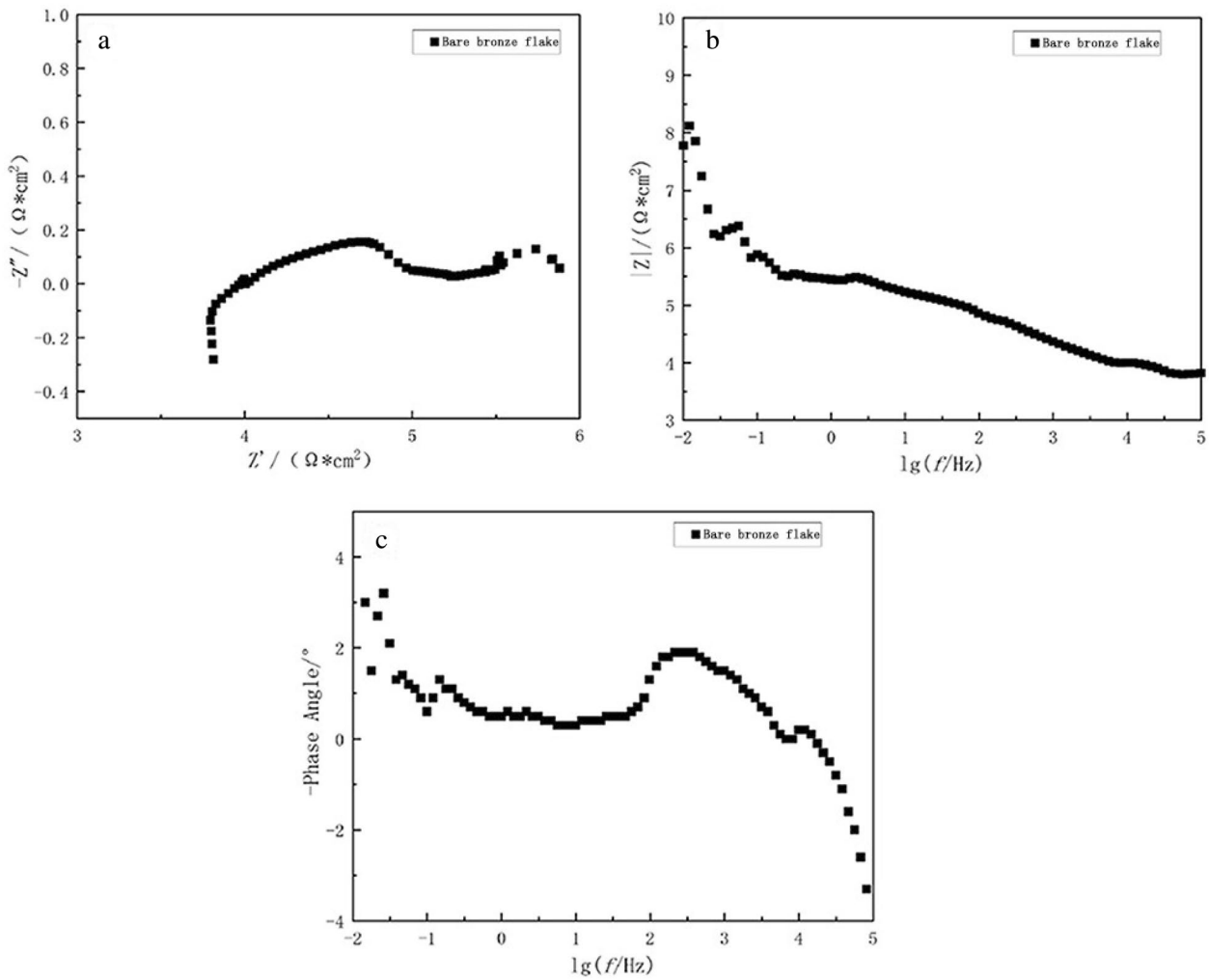

Fig. 6 **a** Nyquist, **b** Bode, and **c** phase diagrams of the bare bronze sheet electrodes immersed in 3.5% NaCl solution

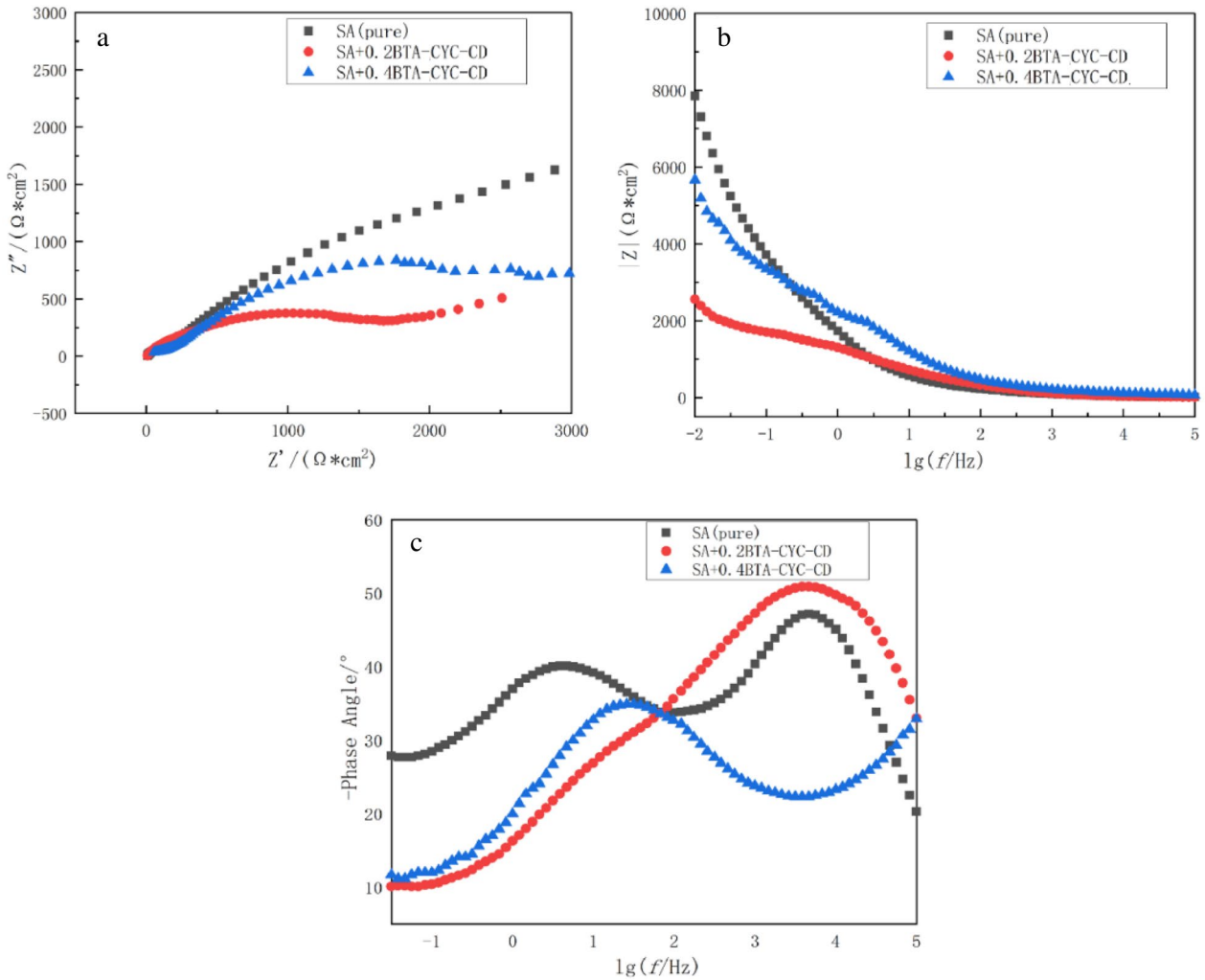

Fig. 7 **a** Nyquist, **b** Bode, and **c** phase diagrams of bronze sheet electrodes coated with gel coatings of various coatings immersed in 3.5% NaCl solution

layer of isolating protective films on the surface of mineralized bronze sheet that separates the mineralized bronze sheet from the external environment and slows down corrosion of the mineralized bronze sheet due to environmental factors within a certain time and to a certain extent. Thus, the anti-corrosion protection effect on the bronze matrix was realized.

SA (pure): pure sodium alginate

SA + 0.2BTA-CYC-CD: The mass ratio of sodium alginate to Cyc-g-β-CD (BTA) is 1:0.2

SA + 0.4BTA-CYC-CD: The mass ratio of sodium alginate to Cyc-g-β-CD (BTA) is 1:0.4

According to the corrosion system of the SA-based Cyc-g-β-CD (BTA) composite coating, the equivalent circuit in Fig. 8 was selected for fitting, where R1, R2, and R3 represent the solution resistance, gel coating resistance, and charge transfer resistance, respectively.

C1 is the membrane capacitance, whereas C2 is the electrical double-layer capacitance between the electrode surface and corrosion medium; the fitting results revealed that the total impedance values were 752.851, 2265, and 3023 Ω for the bare electrode, electrode

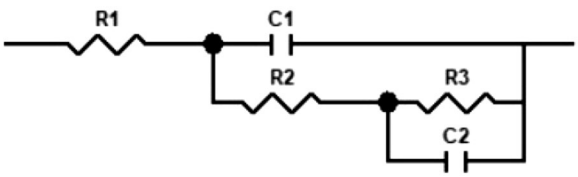

Fig. 8 Equivalent circuit of impedance spectra

coated with pure alginate gel, and electrode coated with Cyc-g-β-CD (BTA), respectively, at a mass ratio of 0.2. The electrode total impedance of the SA gel coated with the Cyc-g-β-CD (BTA) content of 0.4 was 3174 Ω, and the BTA-loaded Cyc-g-β-CD hydrogel coated at the same immersion time point exhibited a superior impedance effect. The impedance effect increased with an increase in the content of cyclic peptide.

The infrared results revealed that Cyc-g-β-CD (BTA) doping could enhance the interaction between the hydrogel mesh layers [15], thereby hindering the progress of the corrosive medium penetrating the hydrogel coating and increasing the charge transfer resistance.

Evaluation of long-term protective effect of coatings

To evaluate the long-term protective effect of the coating, we induced artificial aging on the coated bronze sheet and examined changes in its protective effect through electrochemical analysis.

In the equivalent circuit model shown in Fig. 8, the ideal capacitive element C is replaced by a constant-phase element CPE to better fit the oblate semicircle in the Nyquist diagram. As shown in Fig. 9, the diameter of the capacitive semicircle of coated bronze sheets at high frequencies was large, which indicates the continuity of corrosion inhibition performance. The fitting results revealed that the total impedance values were 2392 Ω and 2464 Ω for uncoated bronze and coated bronze sheets, respectively, which implied that the gel coat can maintain a certain corrosion inhibition performance even under 60 h of high-intensity corrosion. By comparing Fig. 10d and f, we found that no obvious corrosion occurred on the surface of the coated bronze sheet, while red rust appeared on the surface of the uncoated bronze

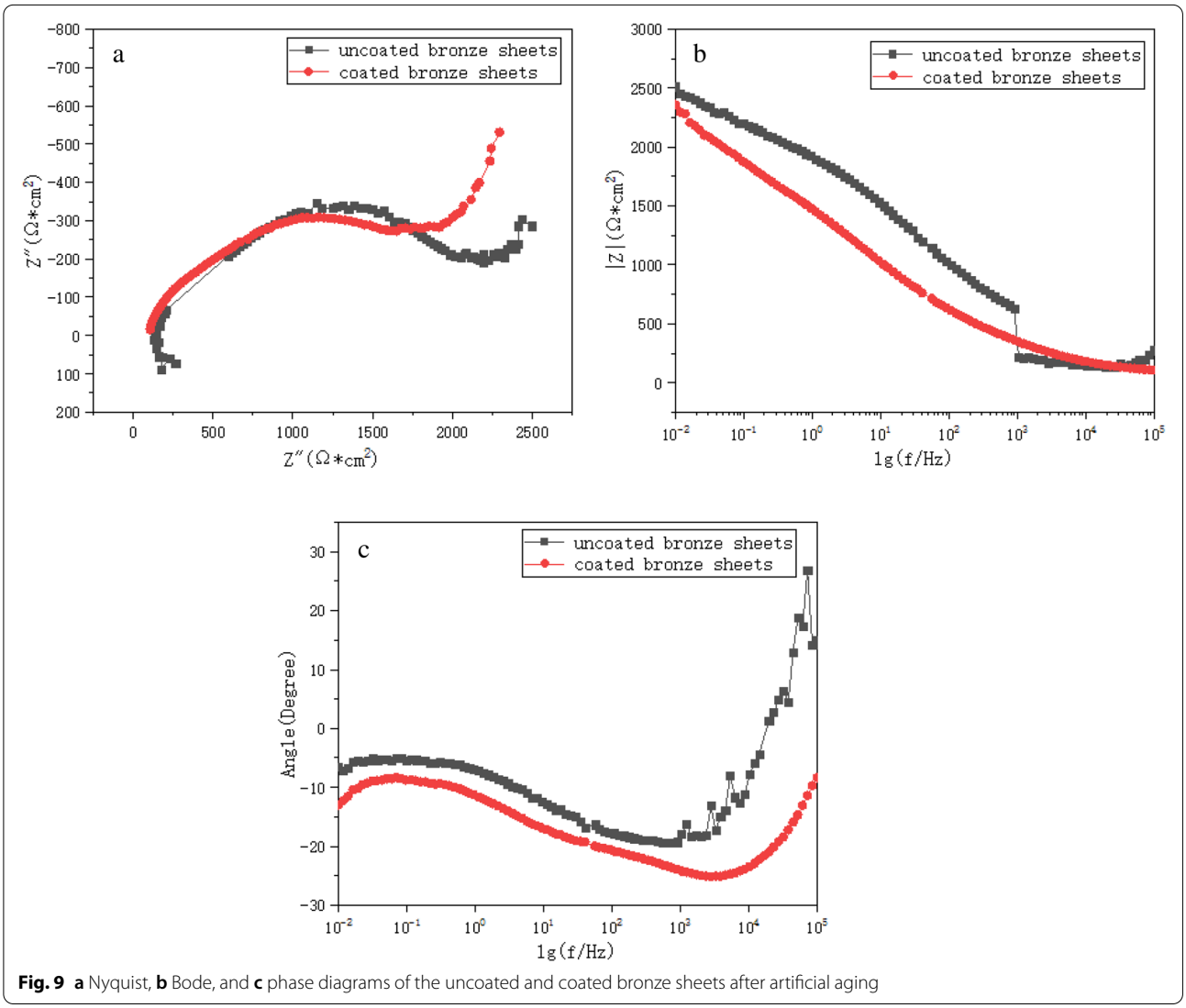

Fig. 9 **a** Nyquist, **b** Bode, and **c** phase diagrams of the uncoated and coated bronze sheets after artificial aging

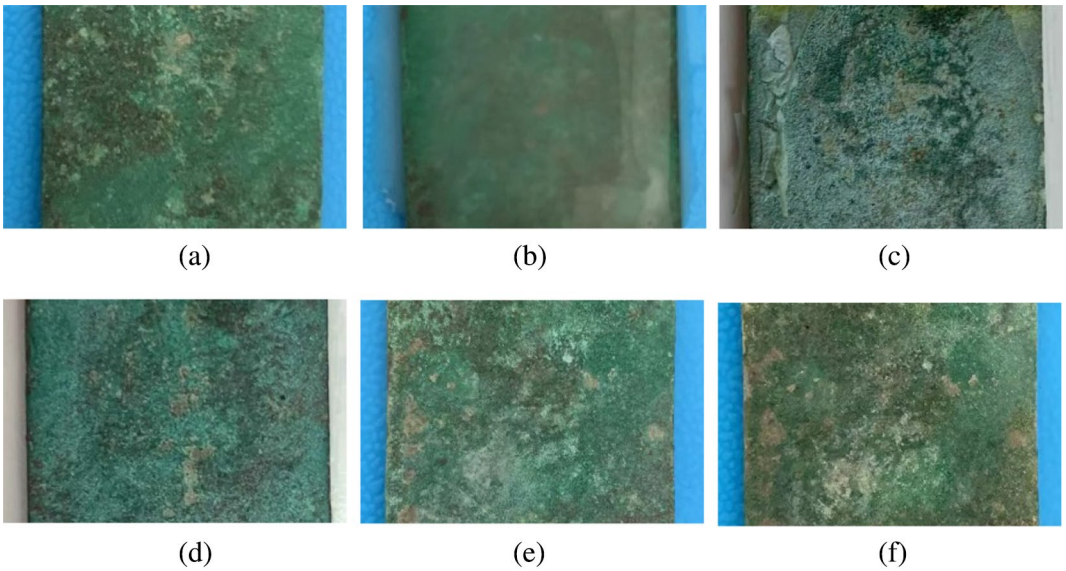

Fig. 10 Coated bronze sheet before and after coating and aging pictures: **a** uncoated bronze sheet; **b** Coated bronze sheet (undried); **c** coated bronze sheet after artificial aging; **d** bronze sheet after removing the deposited coating in (**c**) Uncoated bronze sheet before and after aging: **e** uncoated bronze sheet; **f** uncoated bronze sheet after artificial aging

sheet. As shown in Fig. 10, after artificially aging, the coating was deposited on the surface of the bronze sheet to form a thin film. These results along with the results of electrochemical analysis indicated that the coating has a corrosion inhibition effect.

Conclusion

A gel coating with excellent protection and corrosion inhibition properties was synthesized by grafting and blending BTA into a prepared container by applying vacuum negative pressure, followed by blending alginate sol and Cyc-g-β-CD (BTA) container. The main conclusions derived from this study are as follows:

1. β-Cyclodextrins were successfully aminoacylated through an amidation reaction, and epoxy Cyc was successfully branched onto the aminoacylated β-cyclodextrins through an amino ring opening reaction.
2. The inclusion was stirred under vacuum, and BTA was successfully included in a Cyc-g-β-CD vessel.
3. Infrared results indicated that Cyc-g-β-CD (BTA) was effectively doped in the SA hydrogel.
4. The obtained gel coating blended with a Cyc-g-β-CD container was loaded with BTA, and the obtained samples exhibited excellent coating, film-forming properties, and corrosion resistance with a certain protective capacity.
5. The Cyc-g-β-CD containers were highly dispersed in the coating, and the presence of layered liquid crystals also enhanced the barrier properties of the gel coating to some extent. The physical combination between the gel coating and bronze matrix occupied the mineralized bronze surface dimples as well as the voids of the rust layer. The release of BTA resulted in the reaction with the bronze matrix. The final gel coating could stud onto the mineralized bronze.
6. The doping of BTA-loaded Cyc-g-β-CDs considerably enhanced the interaction between the hydrogel mesh layers, thereby hindering the progress of the corrosive medium penetration into the hydrogel coating. The SA-based BTA-loaded coating of Cyc-g-β-CD composite hydrogel exhibited a certain sheet liquid crystallinity. The network structure inside the gel directly formed a layer of isolation protective films on the surface of the mineralized bronze sheet, separated the mineralized bronze sheet from the external environment, and slowed down the corrosion of mineralized bronze sheets by environmental factors for a certain time and to a certain extent to lend protection to mineralized bronze sheets against corrosion.

Abbreviations
BTA: Benzotriazole; Cyc-g-β-CD: Cyclic-peptide-grafted β-Cyclodextrins; Cyc-g-β-CD (BTA): BTA-loaded Cyc-g-β-CD; SA: Sodium alginate; Cyc: Epoxide Cyc [19]; TGA: Thermogravimetric; DSC: Differential scanning calorimetry; AC: Alternating current.

Acknowledgements
Thanks to the rusted bronze sample provided by Henan Provincal Institute of Cultural Relices and Archaeology.

Author contributions
Z S wrote the main manuscript text and prepared figures. Z Z participated in the preparation of the manuscript data. The other authors helped with the manuscript to some extent. H X revised and guided the manuscript. All authors reviewed, read and approved the final manuscript.

Funding
This research was supported by The National Key Research and Development Program of China (No. 2020YFC1522000).

Availability of data and materials
All data generated or analyzed during this study are included in this published article [and its supplementary information files].

Declarations

Competing interests
The authors declare that there are no conflicts of interest regarding the publication of this paper.

Author details
[1]School of Materials Science and Engineering, Zhengzhou University, Zhengzhou, Henan 450001, People's Republic of China. [2]School of Chemistry, Zhengzhou University, Zhengzhou, Henan 450001, People's Republic of China. [3]Henan Provincial Institute of Cultural Relics and Archaeology, Zhengzhou, Henan 450000, People's Republic of China.

Received: 14 February 2022 Accepted: 26 June 2022
Published online: 25 July 2022

References

1. Wang D, Pan C, Liu Z, Chen K, Chen N. Shuhua Liu, Synergetic effect of two inhibitors for enhanced corrosion protection on the reinforcing steel in the chloride-contaminated carbonated solutions. Constr Build Mater. 2021;286: 122916.
2. Laguzzi G, Luvidi L. Evaluation of the anticorrosive properties of benzotriazole alkyl derivatives on 6% Sn bronze alloy. Surf Coat Technol. 2010;204(15):2442–6.
3. Giuliani C, et al. Chitosan-based coatings for corrosion protection of copper-based alloys: a promising more sustainable approach for cultural heritage applications. Prog Org Coat. 2018;122:138–46.
4. Brandi C. Theory of cultural relics restoration. Italia: Italian Institute of African and Oriental Studies; 1963.
5. Martina S, et al. Long-lasting efficacy of coatings for bronze artwork conservation: the key role of layered double hydroxide nanocarriers in protecting corrosion inhibitors from photodegradation. Angew Chem Int Ed. 2018;57:7380–4.
6. Montemor M, et al. Evaluation of self-healing ability in protective coatings modified with combinations of layered double hydroxides and cerium molibdate nanocontainers filled with corrosion inhibitors. Electrochim Acta. 2012;60:31–40.
7. Fu J, et al. Acid and alkaline dual stimuli-responsive mechanized hollow mesoporous silica nanoparticles as smart nanocontainers for intelligent anticorrosion coatings. ACS Nano. 2013;7(12):11397–408.
8. Mikhail L, et al. Anticorrosion coatings with self-healing effect based on nanocontainers impregnated with corrosion inhibitor. Ferreira. Chem Mater. 2007;19(3):402–11.
9. Lee J, Cho S-W, et al. Mechanically-reinforced and highly adhesive decellularized tissue-derived hydrogel for efficient tissue repair. Chem Eng J. 2021;427: 130926.
10. Ren P, et al. Preparation and evaluation of intelligent corrosion inhibitor based on photo-crosslinked pH-sensitive hydrogels. Mater Lett. 2015;160:480–3.
11. Gu T, et al. A preliminary research on polyvinyl alcohol hydrogel: a slowly-released anti-corrosion and scale inhibitor. J Petrol Sci Eng. 2014;122:453–7.
12. Arya P, Raghav N. In-vitro studies of Curcumin-β-Cyclodextrin inclusion complex as sustained release system. J Mol Struct. 2021;1228: 129774.
13. Akhondi M, Jamalizadeh E. Fabrication of β-Cyclodextrin modified halloysite nanocapsules for controlled release of corrosion inhibitors in self-healing epoxy coatings. Prog Org Coat. 2020;145: 105676.
14. Ge S, Zhao X, Gai Z, et al. Adsorption geometry of glycine on Cu(001) determined with low-energy electron diffraction and scanning tunnelling microscopy. Chin Phys Lett (English version). 2001;18(2):286–8.
15. He F, Wang L, Yang S, et al. Highly stretchable and tough alginate-based Cyclodextrin/Azo-polyacrylamide interpenetrating network hydrogel with self-healing properties. Carbohyd Polym. 2021;256: 117595.
16. Grgur B, Lazić V, Stojić D, Rudolf R. Electrochemical testing of noble metal dental alloys: the influence of their chemical composition on the corrosion resistance. Corros Sci. 2021;184: 109412.
17. Sanchez T, Kurchavova E, Shkirskiy V, et al. Detection and quantification of defect evolution at buried metal-oxide-polymer interface on rough substrate by local electrochemical impedance mapping. Electrochim Acta. 2021;388: 138467.
18. Silva C, et al. The synergistic effect of an imidazolium salt and benzotriazole on the protection of bronze surfaces with chitosan-based coatings. Herit Sci. 2020;8:40.
19. Huang X, Shen C, Chen J, et al. Curing kinetic study of biodegradable amino acid derived epoxy resin. Polym Mater Sci Eng. 2021;25(12):73–6.
20. Medeleanu M, Hadaruga D, Muntean C, et al. Structure-property relationships on recrystallized β-Cyclodextrin solvates: a focus on X-ray diffractometry. FTIR Thermal Anal Carb Polym. 2021;265: 118079.
21. Du L, et al. Quantum chemical and molecular dynamics studies of imidazoline derivatives as corrosion inhibitor and quantitative structure–activity relationship (QSAR) analysis using the support vector machine (SVM) method. J Theor Comput Chem. 2014;13(2):1.
22. Hu S, et al. Quantum chemical analysis on molecular structures and inhibitive properties of imidazoline inhibitors. Zhongguo Shiyou Daxue Xuebao (Ziran Kexue Ban)/J Chin Univ Petrol (Edition of Natural Science). 2011;351:146–50.
23. Turo F, Matricardi P, Meo C, et al. PVA hydrogel as polymer electrolyte for electrochemical impedance analysis on archaeological metals. J Cult Herit. 2019;37:113–20.

Publisher's Note